# INFLUENCE OF REAR-SIDE PASSIVATION ON SOLAR CELL PERFORMANCE OF BOSCO SOLAR CELLS

Karin Krauß, Fabian Fertig, Johannes Greulich, Florian Clement, Daniel Biro, Ralf Preu, Stefan Rein
Fraunhofer Institute for Solar Energy Systems ISE, Heidenhofstr. 2, D-79110 Freiburg, Germany

ABSTRACT: The recently introduced BOSCO ("Both Sides Collecting and Contacted") solar cell exhibits emitter regions on front and rear side, which are interconnected by diffused vias. This allows double-sided collection of carriers in the base and bifacial operation while supporting standard module interconnection technology. Since the BOSCO cell's rear side exhibits *p*-doped as well as highly $n^+$-doped surfaces the dielectric used as rear-side passivation needs to be suitable to passivate both polarities. This work compares the passivation of the BOSCO cell's rear side by a PECVD aluminium oxide ($AlO_x$) and a thermally grown silicon oxide ($SiO_2$). A difference in efficiency of up to $\Delta\eta = 0.5\ \%_{abs}$ occurs between BOSCO cells with $AlO_x$ and $SiO_2$ passivation, with the $AlO_x$ passivated solar cells achieving better cell performance. The difference in efficiency is dominated by a loss in fill factor of up to $\Delta FF = 1.6\ \%_{abs}$ for cells with $SiO_2$ passivation compared to $AlO_x$ passivated cells. An investigation of the suns-$V_{oc}$ characteristics shows that this loss is mainly caused by increased recombination at lower injection, which strongly affects the pseudo fill factor. This work shows that the choice of rear-side passivation is essential to optimize the performance of BOSCO solar cells.

Keywords: BOSCO, bifacial, passivation, double-sided collection, multicrystalline silicon

## 1 INTRODUCTION

The BOSCO ("*Bo*th *S*ides *CO*llecting and *CO*ntacted") solar cell [1, 2] features a double-sided emitter and a grid on both sides as sketched in Fig. 1. The front- and rear-side emitter areas are interconnected by diffused vias. For the rear-side contact grid the emitter is disconnected. The double-sided emitter allows carrier collection on either side and, therefore, supports the use of lower diffusion length material such as multicrystalline silicon (mc-Si) [2]. Furthermore, the layout of the front- and rear-side grid allows for bifacial application while supporting standard module interconnection technology. Compared to Al-BSF cells a significant advantage in monofacial efficiencies has been demonstrated [2, 3]. Furthermore, it has been shown that the BOSCO cell concept is a promising candidate to enable bifacial application also for low-to-medium diffusion length material such as mc-Si [2, 3]. A principle process flow of the BOSCO cell concept with a complexity similar to a typical PERC processing route has been introduced [3]. Due to the interdigitated structure of the rear-side emitter and base regions, the passivation layer deposited on the rear side has to passivate both a *p*-type and a highly-doped $n^+$-type surface. Thin thermal silicon oxide ($SiO_2$) films capped with silicon nitride have been shown to achieve low surface recombination velocities on the rear side of *p*-type PERC cells [4], simultaneously achieving low front-side $n^+$-type emitter recombination [4]. Therefore, $SiO_2$ seems to be a promising candidate for the passivation of BOSCO cells, where *p*-type and highly doped $n^+$-type surfaces need to be passivated by the same layer. Aluminium oxide ($AlO_x$) deposited by plasma-enhanced chemical vapour deposition (PECVD) is known to be well-suited for the passivation of *p*-type doped silicon [5], due to a low interface defect density and fixed negative charges at the interface. Furthermore, PECVD $AlO_x$ has been reported to yield good passivation quality on $n^+$-emitters [6].

In this work, we compare thin thermally grown $SiO_2$ and PECVD $AlO_x$ for the use as rear-side passivation of BOSCO cells.

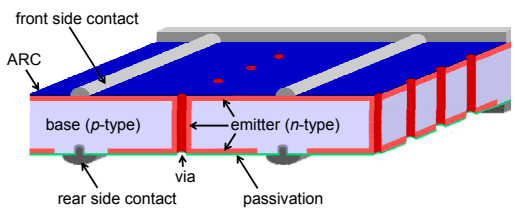


**Figure 1** Sketch of the BOSCO cell structure. Illustration is taken from Ref. [2]

## 2 EXPERIMENTAL

For this work, BOSCO cells processed on 15.6×15.6 cm² block-cast mc-Si wafers with varying base resistivity and purity are investigated. The investigated materials include upgraded metallurgical-grade (UMG) Si with a feedstock purity of 5N (i.e., 99.999 % pure silicon) as well as electronic-grade (EG) Si with a purity of 9N.

Fig. 2 depicts the process flow for the BOSCO cells with a variation of the rear-side passivation layer. The key properties of the BOSCO process are described in Ref. [3]. Prior to surface texturing, vias are drilled using an IR laser. After a rear side polish, which may not be needed once the BOSCO process is optimized for bifacial illumination, a diffusion barrier is deposited in order to

| BOSCO $AlO_x$ | BOSCO $SiO_2$ | BOSCO w/o passivation |
|---|---|---|
| drill vias | drill vias | drill vias |
| texture | texture | texture |
| polish rear side | polish rear side | polish rear side |
| deposit diffusion barrier | deposit diffusion barrier | deposit diffusion barrier |
| diffusion + PSG etch | diffusion + PSG etch | diffusion + PSG etch |
| rear side PECVD $AlO_x$ | thermal oxidation | |
| rear side $SiO_x/SiN_x$ capping | rear side $SiO_x/SiN_x$ capping | |
| front side ARC | front side ARC | front side ARC |
| rear side print | rear side print | rear side print |
| front side print | front side print | front side print |
| firing | firing | firing |
| formation of rear side contact | formation of rear side contact | formation of rear side contact |

**Figure 2** Principle process flow for the production of BOSCO solar cells with a variation of the passivation schemes.

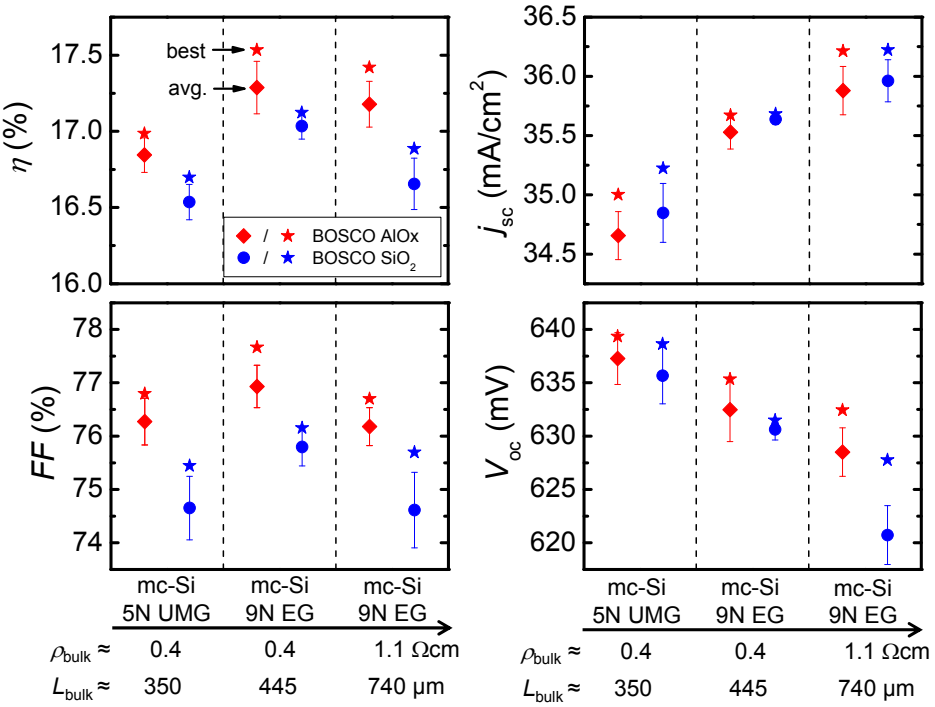


**Figure 3** Illuminated *I-V* parameters for front-side illumination of the processed BOSCO cells with $AlO_x$ and $SiO_2$ rear-side passivation. The cells have been measured on a non-reflecting chuck. Cell areas are $A_{cell}$ = 15.6 × 15.6 cm$^2$.

obtain the structured emitter on the rear side. In this experiment, the diffusion barrier is formed by a PECVD silicon oxide ($SiO_x$) with a screen-printed etch resist lacquer and subsequent wet chemical oxide etch-off and stripping of the lacquer. After the diffusion, the diffusion barrier is removed in the PSG etch. The rear-side passivation has been varied between

(i) PECVD $AlO_x$,
(ii) thermally grown $SiO_2$ and
(iii) no rear-side passivation at all.

The thin $SiO_2$ film is thermally grown during an oxidation process at a plateau temperature of 800°C in an inline walking string furnace [7]. Note that for this group the front-side emitter is passivated with $SiO_2$ as well. Both passivation layers, the $AlO_x$ and the $SiO_2$, are stacked with a capping layer consisting of a PECVD $SiO_x$ and a PECVD silicon nitride ($SiN_x$). On the front side, a PECVD $SiN_x$ is deposited as an anti-reflective coating (ARC). For the cells passivated with $SiO_2$, the thickness of the ARC is adapted considering the thin $SiO_2$ layer which is deposited on the front side as well. After screen printing of the rear and front side and subsequent firing, the rear-side contact is formed with laser-fired contacts (LFC) [8, 9].

## 3 IMPACT ON CELL PERFORMANCE

### 3.1 *I-V* parameters

Illuminated *I-V* parameters have been measured under front-side illumination on a non-reflecting chuck. The results for the passivated cells are shown in Fig. 3, the results for cells without passivation will be discussed later within the fill factor analysis. On all materials, cells with $AlO_x$ passivation yield higher efficiencies than cells passivated with $SiO_2$. The difference in-between both groups is $\Delta\eta$ = 0.3 to 0.5 $\%_{abs}$ or $\Delta\eta$ = 1.5 to 2.1 $\%_{rel}$, respectively. For the UMG Si cells with $AlO_x$ passivation, the open-circuit voltage is increased by $\Delta V_{oc}$ = 0.3 $\%_{rel}$ and the short-circuit current density is reduced by $\Delta j_{sc}$ = -0.6 $\%_{rel}$, while the fill factor is increased by $\Delta FF$ = 1.8 $\%_{rel}$ compared to cells with $SiO_2$ passivation. For the EG Si materials, the fill factor is increased by $\Delta FF$ = 1.5 $\%_{rel}$ for the low resistivity and by $\Delta FF$ = 3.0 $\%_{rel}$ for the high base resistivity material, respectively, both representing the dominant difference in the *I-V*-parameters between $AlO_x$ and $SiO_2$ passivated cells. Therefore, the lower efficiency of the cells with $SiO_2$ passivation compared with $AlO_x$ passivation can mainly be attributed to losses in fill factor for all materials.

### 3.2 Fill factor and suns-$V_{oc}$ analysis

In order to investigate the differences of the groups in fill factor in more detail, the pseudo fill factor and the fill factor differences between the pseudo fill factor and the ideal fill factor $FF_0$ will be investigated. Series resistances are assumed to be lumped in this analysis so that the *pFF* can be considered to be free from losses due to series resistances [10]. The ideal fill factor is calculated from the ideal *I-V*-curve and is therefore free from losses due to series resistance and recombination in the space charge region [10, 11]. Hence, the fill factor difference $FF_0$-*pFF* quantifies fill factor losses due to recombination in the space charge region and low shunt resistances [10].

Fig. 4 shows the pseudo fill factor and the fill factor difference $FF_0$-*pFF* of BOSCO cells with $AlO_x$ and $SiO_2$ passivation, respectively, and BOSCO cells without any rear-side passivation. On all materials, cells with $AlO_x$ passivation yield the highest *pFF* and the lowest values

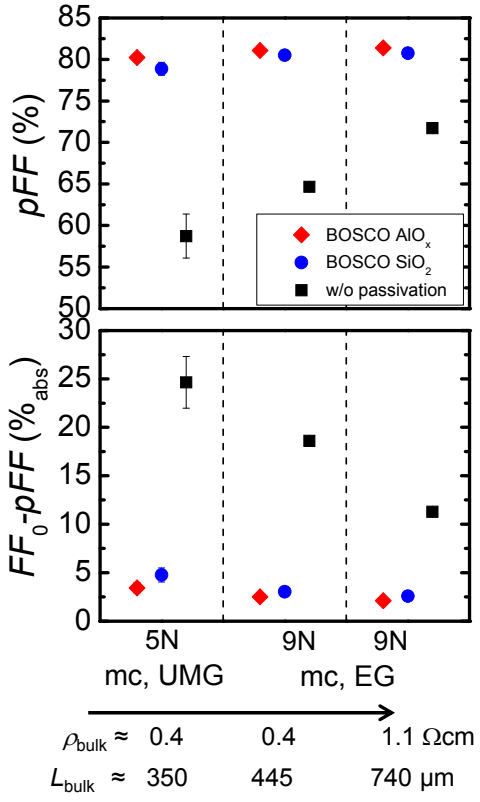


**Figure 4** Pseudo fill factor and fill factor difference between ideal fill factor and pseudo fill factor for all materials and cells with $AlO_x$, $SiO_2$ and without passivation.

for $FF_0$-$pFF$. The difference in pseudo fill factor to cells with $SiO_2$ passivation is $\Delta pFF = 0.6\ \%_{abs}$ for the EG Si materials and $\Delta pFF = 1.4\ \%_{abs}$ for the UMG Si material. Therefore, the fill factor difference $FF_0$-$pFF$ of the cells with $AlO_x$ passivation is decreased by $\Delta(FF_0\text{-}pFF) = 0.5$ and 1.3 $\%_{abs}$ for the EG Si and the UMG-Si, respectively, compared to the cells with $SiO_2$ passivation. For the cells without passivation the $pFF$ is drastically decreased to $pFF = 71.7\ \%$ for the high resistivity and $pFF = 64.7\ \%$ for the low resistivity EG-Si, respectively, and $pFF = 58.7\ \%$ for the UMG-Si material. In this case, the $pFF$ is affected by very low shunt resistances of $R_p < 200\ \Omega cm^2$ which are observed on all materials for cells without rear-side passivation.

To analyze the influence of the passivation on $pFF$ in more detail, suns-$V_{oc}$ characteristics [12] of the cells passivated with $AlO_x$ and $SiO_2$ and the cells without passivation are compared. In Fig. 5 suns-$V_{oc}$ characteristics of a representative BOSCO cell for each material passivated with $AlO_x$, $SiO_2$ and no passivation are shown. For illumination levels below $E = 0.1$ suns, the open-circuit voltage for cells passivated with $SiO_2$ drops more strongly than for cells with $AlO_x$ passivation. Hence, the recombination for low illumination levels is higher for cells with $SiO_2$ passivation than for cells with $AlO_x$ passivation. In case of the cells without passivation, the recombination is even higher, leading to a strong drop in $V_{oc}$ at illumination intensities below $E \approx 0.3$ suns.A possible explanation for this behavior might be re-injection of electrons at the rear-side *pn*-junction, that causes an enhanced sensitivity of cell performance to the

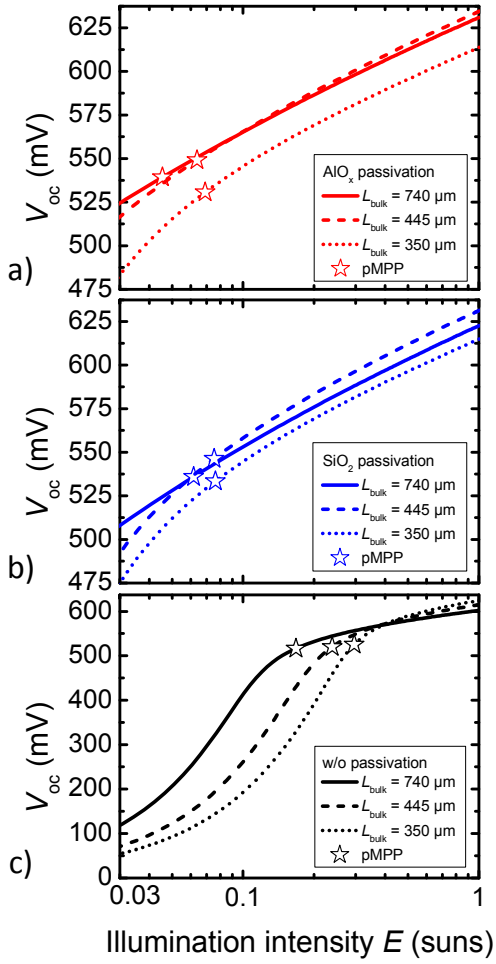


**Figure 5** Suns-$V_{oc}$ curves of BOSCO cells with a) $AlO_x$ passivation b) $SiO_2$ c) without passivation.

passivation quality of the rear-side passivation. Further investigations are on-going.

## 4 CONCLUSION

Solar cell results on mc-Si materials with an $AlO_x$ and a $SiO_2$ passivation on the rear side have been presented. The cells passivated with $AlO_x$ exhibit the highest efficiencies with a difference in efficiency of $\Delta\eta = 0.3$ to 0.5 $\%_{abs}$ compared to cells with $SiO_2$ passivation. The difference in efficiency is mainly attributed to a loss in fill factor. An in-depth analysis of the pseudo fill factor via discussion of the suns-$V_{oc}$ characteristics shows that the pseudo fill factor of the cells with $SiO_2$ passivation is strongly affected by an inferior passivation quality, due to increased recombination in the cell at low illuminations levels. Therefore, we identify $AlO_x$ as the superior passivation for the BOSCO cell concept.

## ACKNOWLEDGEMENTS

This work has been supported by the Fraunhofer Society within the project SiliconBeacon. K. Krauß

gratefully acknowledges the scholarship of the German Federal Environmental Foundation ("Deutsche Bundesstiftung Umwelt").

REFERENCES

[1] F. Clement, "Die Metal Wrap Through Solarzelle - Entwicklung und Charakterisierung," Ph.D. Thesis, Fakultät für Angewandte Wissenschaften, Universität Freiburg.

[2] F. Fertig, K. Krauß, J. Greulich, F. Clement, D. Biro, R. Preu, S. Rein, "The BOSCO solar cell - a both sides collecting and contacted structure," *Phys. Stat. Sol. (RRL), Vol. 8, pp. 381-384, 2014.*

[3] F. Fertig, J. Greulich, K. Krauß, F. Clement, D. Biro, R. Preu, and Rein S, "The BOSCO Solar Cell: Simulation and Experiment," *IEEE J. Photovoltaics, Vol. 4*, no. 5, pp. 1243–1251, 2014.

[4] S. Mack, U. Jager, G. Kastner, E. A. Wotke, U. Belledin, A. Wolf, R. Preu, and D. Biro, "Towards 19% efficient industrial PERC devices using simultaneous front emitter and rear surface passivation by thermal oxidation," *Proceedings of the 35th IEEE PVSEC, Honolulu, 2010*, pp. 34–38.

[5] P. Saint-Cast, D. Kania, M. Hofmann, J. Benick, J. Rentsch, and R. Preu, "Very low surface recombination velocity on p-type c-Si by high-rate plasma-deposited aluminum oxide," *Appl. Phys. Lett,* vol. 95, no. 15, p. 151502, 2009.

[6] S. Duttagupta, F.-J. Ma, S. F. Lin, T. Mueller, A. G. Aberle, and B. Hoex, "Progress in Surface Passivation of Heavily Doped n-Type and p-Type Silicon by Plasma-Deposited AlOx/SiNx Dielectric Stacks," *IEEE J. Photovoltaics*, vol. 3, no. 4, pp. 1163–1169, 2013.

[7] D. Biro, G. Emanuel, R. Preu, and G. Willeke, "High capacity walking string diffusion furnace," *Proceedings of PV in Europe, Rome, 2002*, pp. 303–306.

[8] E. Schneiderlöchner, R. Preu, R. Lüdemann, and S. W. Glunz, "Laser-fired rear contacts for crystalline silicon solar cells," *Prog Photovoltaics*, vol. 10, pp. 29–34, 2002.

[9] A. Mohr, S. Wanka, A. Stekolnikov, M. Scherff, R. Seguin, P. Engelhart, C. Klenke, J. Y. Lee, S. Tardon, S. Diez, J. Wendt, B. Hintze, R. Hoyer, S. Schmidt, J. W. Müller, and P. Wawer, "Large area solar cells with efficiency exceeding 19% in pilot series designed for conventional module assembling," *Energy Procedia*, vol. 8, pp. 390–395, 2011.

[10] J. Greulich, M. Glatthaar, and S. Rein, "Fill factor analysis of solar cells' current-voltage curves," *Prog. Photovolt: Res. Appl,* vol. 18, no. 7, pp. 511–515, 2010.

[11] M. A. Green, *Solar Cells Operating Principles, Technology and System Applications*: University of New South Wales P.O. Box 1 Kensington, NSW 2033, 1986.

[12] R. A. Sinton and A. Cuevas, "A quasi-steady-state open-circuit voltage method for solar cell characterization," *Proceedings of the 16th EUPVSEC, Glasgow, 2000*, pp. 1152–1155.